Immunologic Research (2019) 67:1–11
https://doi.org/10.1007/s12026-019-9066-3

REVIEW

Macrophage phenotype bioengineered by magnetic, genetic, or pharmacologic interference

Jarek Wosik[1,2] · Martha Suarez-Villagran[1,3] · John H. Miller Jr[1,3] · Rafik M. Ghobrial[4,5] · Malgorzata Kloc[4,5,6]

Published online: 16 January 2019

Abstract

In all eukaryotes, the cell shape depends on the actin filament cytoskeleton, which is regulated by the small GTPase RhoA. It is well known that the cell shape determines cell function and behavior. Inversely, any change in the cell behavior and/or function reverberates at the cell shape. In this review, we describe how mechanical/magnetic, genetic, or pharmacologic interference with the actin cytoskeleton enforces changes in cell shape and function and how such techniques can be used to control the phenotype and functions of immune cells such as macrophages and to develop novel anti-cancer and anti-rejection clinical therapies.

Keywords Macrophage · RhoA · Actin · Magnetic field · Transplantation · Cancer

Introduction

Multicellular organisms, including humans, consist of two different, in the very broad sense, types of cells: interconnected cells, which are part of an ensemble of similar cells of the same origin that together carry out specific function(s), and independent/separate cells that function individually or in unison with other individual cells of the same or different types. A good example of the "interconnected" cell type is epithelial or endothelial tissue, which is a layer of cells lining the body surface or various body organs and cavities, respectively. The cells comprising epithelium or endothelium are interconnected by the intercellular junctions, have a clearly defined shape and apical/basal polarity, and are immotile (Fig. 1a, b).

The loss of intercellular connections and cell polarity and acquisition of motility are the hallmark events in cancer development [1]. An example of the "independent" cell type is cells of the immune system, such as macrophages. These cells are not physically connected to each other, have a dynamic shape, are highly motile, and function either individually or in unison with other macrophages or other types of immune cells (Fig. 1c).

Shape, polarity, and functions of macrophages

Macrophages are crucial for innate and adaptive immune response and organ and tissue homeostasis. In addition, the tumor-associated macrophages promote cancer development [2–4]. Macrophages are also major players in the long-term (chronic) rejection of transplanted organs that present a major and so far incurable problem in clinical transplantation [5–7]. Macrophages activated by the transplantation of foreign (non-self, allo) organs infiltrate allograft and accumulate around its blood vessels, promoting vessel occlusion and fibrosis, which lead to organ starvation and deterioration of organ integrity [6, 8]. Depending on the shape, metabolism, and function, the macrophages are divided into three different subtypes: (1) slightly elongated, naïve/unactivated

✉ Jarek Wosik
jarek@uh.edu

✉ Malgorzata Kloc
mkloc@houstonmethodist.org

1 Electrical and Computer Engineering Department, University of Houston, Houston, TX 77204, USA

2 Texas Center for Superconductivity, University of Houston, HSC Bldg., Rm. 202, Houston, TX 77204-5002, USA

3 Physics Department, University of Houston, Houston, TX, USA

4 The Houston Methodist Research Institute, Houston, TX 77030, USA

5 Department of Surgery, The Houston Methodist Hospital, 6550 Fannin St., Houston, TX 77030, USA

6 M.D. Anderson Cancer Center, Department of Genetics, The University of Texas, Houston, TX 77030, USA

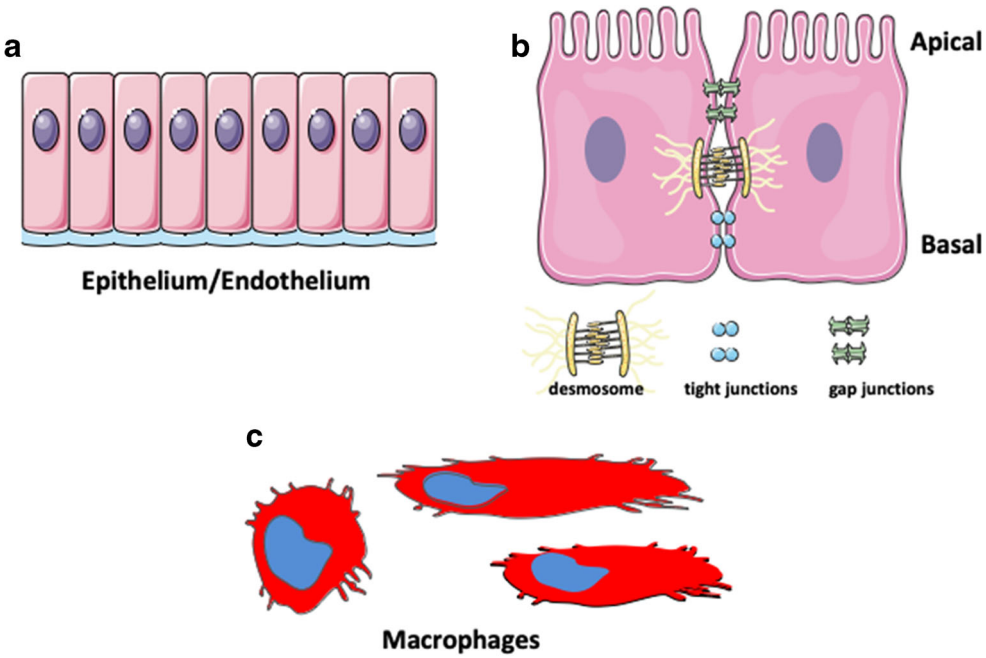

Fig. 1 Diagram of interconnected versus independent cells. **a** Epithelial/endothelial cells have defined shape, apical and basal polarity, and are interconnected to each other into a tight layer. **b** Types of cell junctions connecting endothelial or epithelial cells. **c** The immune cells such as macrophages are independent from each other and have variable shape

M0 macrophages; (2) round, pro-inflammatory M1 macrophages that fight infections; and (3) elongated, anti-inflammatory M2 macrophages that play a major role in tissue repair and wound healing (Fig. 2) [2, 4, 9–14]. Pro-inflammatory M1 macrophages produce the bactericidal molecule, an inducible nitric oxide synthase, and anti-inflammatory M2 macrophages produce the pro-healing enzyme arginase 1 (Arg-1). The M0 and M2 macrophages have very defined polarity with an expanded front and elongated tail (Fig. 2).

Actin filaments and RhoA pathway regulation of macrophage shape and structuring of macrophage organelles

The macrophage shape depends on the actin filaments, which form through the energy/ATP- and Ca^{+2}-dependent polymerization of the globular actin (G actin) into the filamentous (F) actin [15, 16]. During macrophage movement, the wave of actin reorganization and polymerization is especially prominent in the front of the cell, and this is where the energy-

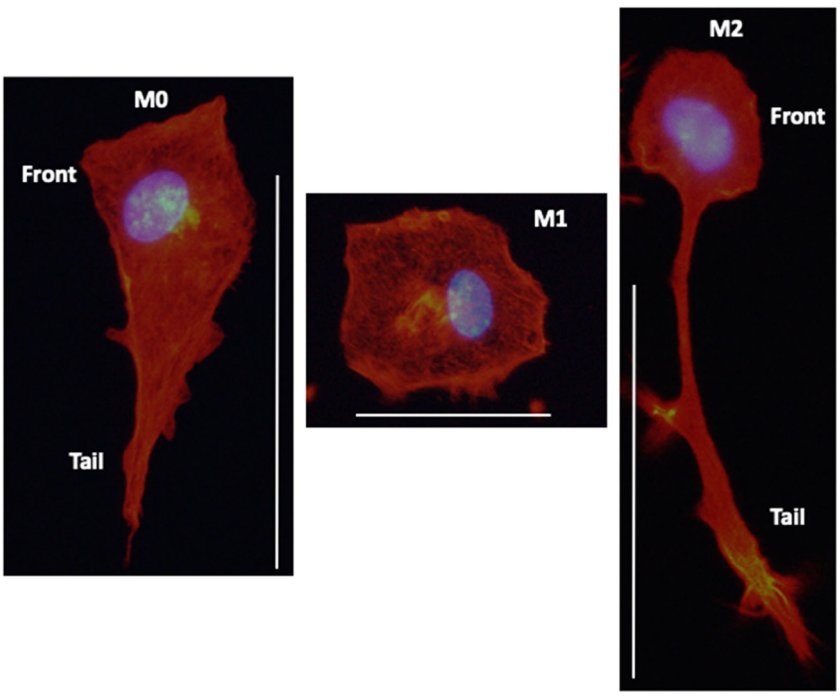

Fig. 2 Different shapes of mouse peritoneal macrophages. **a** Naïve/unactivated M0 macrophage is slightly elongated with well-defined front (containing nucleus) and tail. **b** Pro-inflammatory M1 macrophage is round. **c** Anti-inflammatory M2 macrophage is elongated. Macrophages were stained with rhodamine-phalloidin to visualize actin (red) and with DAPI to visualize nuclei (blue). Bar is equal to 50 μm

producing mitochondria accumulate [17–19] (Fig. 3a). The whole process of actin polymerization/depolymerization depends on the small GTPase RhoA and its downstream effector, the p160 kinase ROCK [6, 20] (Fig. 3b). In turn, the RhoA/ROCK activity is regulated by the subset of guanine exchange factors, RhoA GEFs [21–25] (Fig. 3c).

Besides orchestrating the cell shape and movement, actin and the RhoA pathway are also involved in the organization and functions of subcellular organelles such as the Golgi complex and endocytic and exocytic vesicular pathways [26–33], which orchestrate engulfment of the external compounds and molecules, vesicular transport of compounds and molecules within the cell and to the cell surface, and receptor recycling (Fig. 4) [34].

The effects of genetic and pharmacologic interference with the actin/RhoA pathway on macrophage shape and functions

It is well established experimentally that the isolated, naïve, rodent M0 macrophages can be induced (polarized) in vitro into M1 or M2 phenotype by supplementation of the culture medium with lipopolysaccharide and interferon gamma or with interleukin-4 and interleukin-13, respectively [10–12] (Fig. 5). We showed recently that the shape and phenotype of rodent macrophages could also be bioengineered by inhibition of the RhoA pathway. The inhibition of RhoA/ROCK activity using ROCK inhibitors, macrophage-specific deletion of RhoA, or inhibition of RhoA GEFs employing Rhosin or Y16 inhibitors causes extreme elongation (so-called hummingbird phenotype) of M0 and M2 (but not M1) macrophages and disorganization and collapse of the actin-dependent organization of the Golgi complex and the receptor recycling (Figs. 4 and 6) [10–13, 35, 36].

We showed that the extreme elongation of macrophages was caused by the accumulation of actin-associated focal adhesions in the macrophage tail, which in turn disabled tail detachment from the substrate while the front of the macrophage was moving forward [10–12, 35]. These phenotypical changes of macrophages had a profound effect on macrophage function in vivo in rodent heart transplantation models. The RhoA-interfered macrophages were unable to move into the transplanted hearts and were unable to mount the long-term immune response culpable for chronic (long-term) rejection of the transplants [35]. Interestingly, the interference with the mitochondrial functions and ATP/ADP homeostasis reversed RhoA interference-induced elongation and shortened M0 and M2 macrophages [36]. However, further studies are needed to establish the effects of mitochondrial interference on macrophage function in vivo in rodent transplantation model systems.

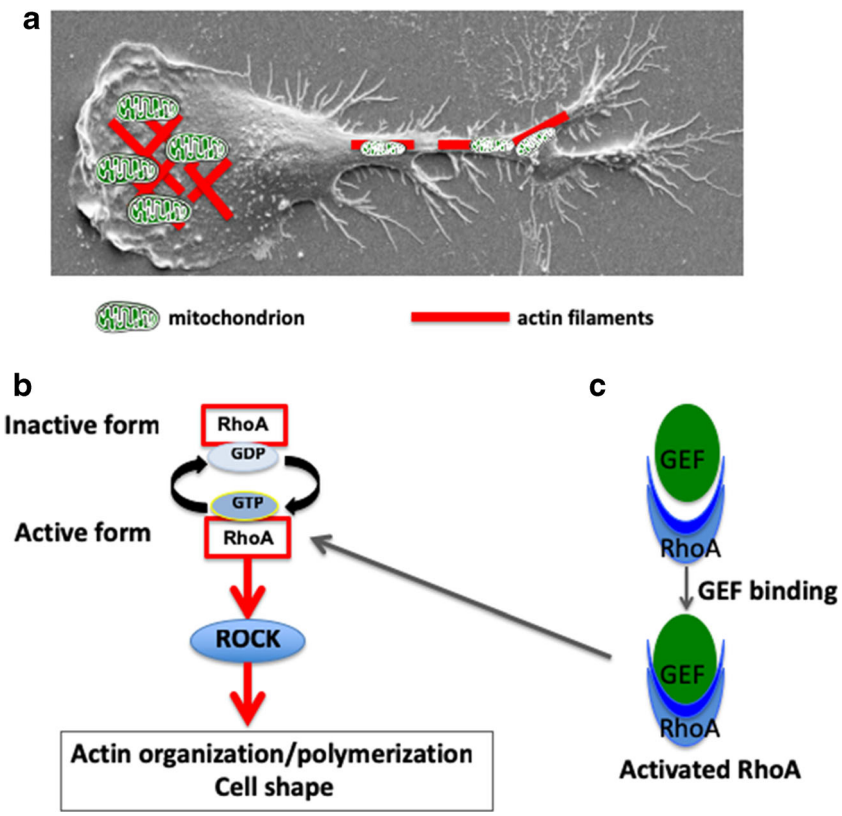

Fig. 3 Actin cytoskeleton is controlled by RhoA pathway and mitochondria. **a** During macrophage movement, there is reorganization of actin cytoskeleton especially in the front of cell where also mitochondria accumulate to deliver energy/ATP. The drawing of mitochondria (green) and actin filaments (red) is superimposed on the scanning electron microscopy image of real mouse peritoneal macrophage. **b** Actin organization/polymerization is regulated by small GTPase RhoA and its downstream effector ROCK kinase. **c** RhoA activity is regulated by RhoA-specific guanine exchange factors (GEFs). (Panel **a** is modified from the panel a of Fig. 2 [11]

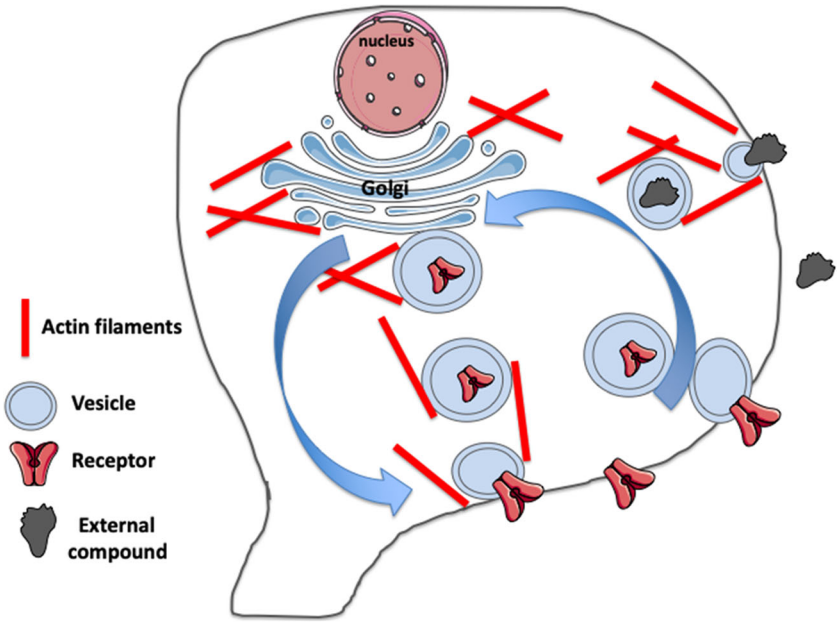

Fig. 4 Diagram of actin-dependent structures such as Golgi complex and endocytosis/exocytosis vesicular pathway. Golgi complex consists of stacks of membranous cisternae and produces endocytic vesicles, which engulf external compounds and transport them into the cell interior for digestion/degradation, and exocytic vesicles, which transport various molecules such as receptor to the cell membrane. The combination of exocytosis and endocytosis pathway recycles various molecules such as surface receptors from the Golgi to the cell membrane and back. Ultrastructure and organization of the Golgi complex and exocytic/endocytic vesicle formation, structure, and functions are actin dependent

The effects of genetic and pharmacologic interference with actin/RhoA pathway on macrophage organelles

Although macrophage elongation is a readily noticeable effect of genetic or pharmacologic interference with the RhoA pathway, there are also other profound changes noticeable at the subcellular/organellar level. As in all eukaryotic cells, the organization and function of the subset of macrophage organelles depend on the actin cytoskeleton. One such organelle is the Golgi complex and the Golgi-dependent exocytic and endocytic vesicular pathways. The Golgi complex consists of stacks of membranous cisternae, which collect proteins produced by the endoplasmic reticulum. Some of these proteins are, after being modified within the Golgi, packed into vesicles pinching off the Golgi cisternae and transported to the cytoplasm for internal use [28]. Other types of proteins, such as surface receptors or secreted cytokines, are transported within the exocytic (secretory) vesicles to the cell surface, where they become incorporated into the plasma membrane or they are secreted outside the cell, respectively (Fig. 4). In the reverse process, the endocytic vesicles, which form at the cell surface, engulf the used-up receptors or exterior compounds and move them back to the Golgi for recycling or to the cytoplasm/lysosomes for further processing/digestion, respectively (Fig. 4). The structure of the Golgi complex and the formation and transport of exocytic and endocytic vesicles depend on actin filaments [26, 27, 30–34, 37]. We showed that genetic or pharmacologic interference with the RhoA pathway dissipates the macrophage Golgi complex and interferes with the endocytic pathway and recycling of macrophage receptors that home macrophages to the transplanted heart [35, 36, 38, 39]. This, in turn, prevents macrophage movement into the transplanted heart and prevents chronic rejection [13, 35].

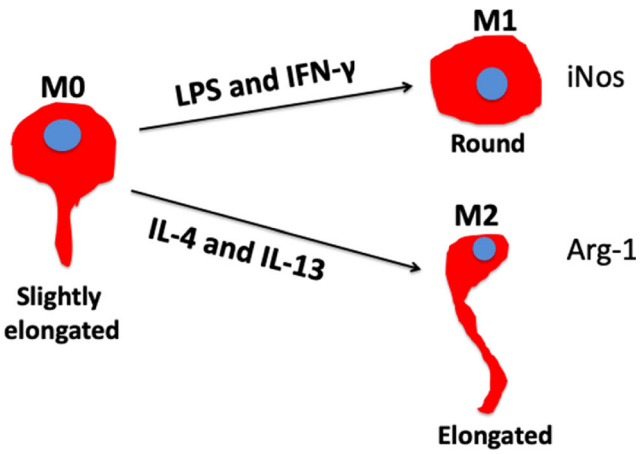

Fig. 5 In vitro polarization of naïve/unactivated M0 macrophages. Addition of LPS and IFN-γ or IL-4 and IL-13 to the culture medium polarizes M0 macrophages into M1 or M2 phenotype, respectively. M1 macrophages produce pro-inflammatory molecule iNOS and M2 macrophages produce anti-inflammatory Arg-1

The effects of magnetic force on macrophages

Recent studies showed that macrophage elongation could also be enforced by surface topography and grating, which modulate

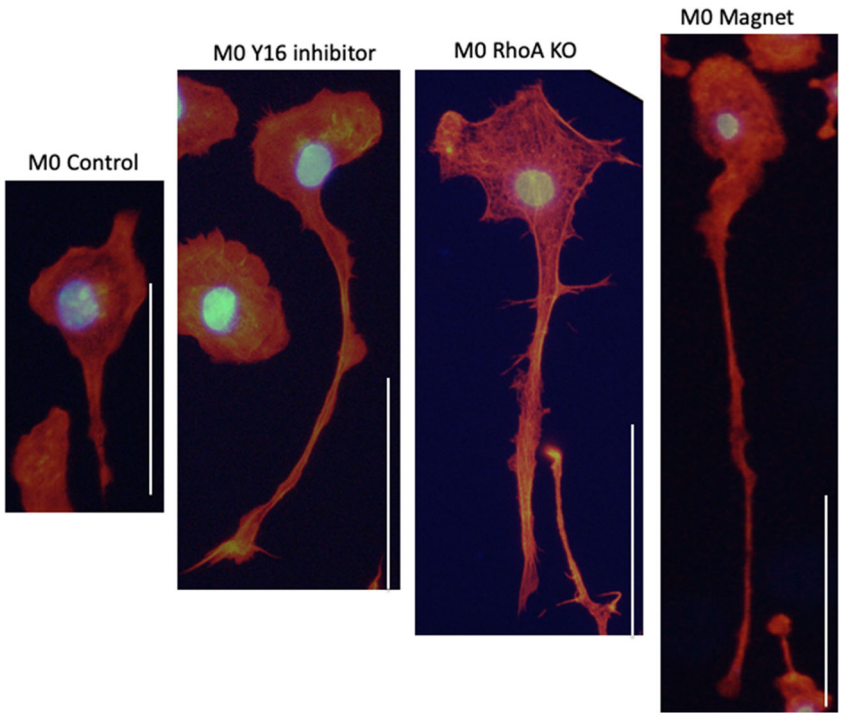

Fig. 6 Elongation of macrophages after various treatments. **a** M0 untreated mouse macrophage is slightly elongated. **b** Treatment with RhoA GEF inhibitor or **c** macrophage-specific deletion of RhoA or **d** exposure to the magnetic field gradient causes extreme macrophage elongation (hummingbird phenotype). Macrophages were stained with rhodamine-phalloidin to visualize actin (red) and with DAPI to visualize nuclei (blue). Bar is equal to 50 μm

actin organization through mechanical forces' effect on the cell membrane, calcium ions, and calcium channel receptors [38–40]. Such conversion of mechanical forces to biochemical interactions is referred to as mechanotransduction. Following this approach, we have explored a case in which the external force acting on macrophages was created by applying a magnetic field. We found that when a nonuniform magnetic field gradient is exerted on macrophages, then resulting mechanical forces affect the cells through the cytoskeleton architecture and mechanoreceptors, inducing macrophage elongation [41].

In the experiments with cultured macrophages, we have used a pair of rare-earth (neodymium-iron-boron) permanent magnets to generate the nonuniform magnetic field pattern. All simulations of the DC magnetic field-magnitude pattern, resulting from its magnetic field gradient and magnetic force lines' distributions, were carried out using a full-wave, finite element-based software package ANSYS (Maxwell) [42]. Mathematics and DC/AC modules of this software were employed for the calculations. To create as large as possible a gradient above the planar magnets' surface, an NS-SN antiparallel magnetization configuration was arranged, as shown in Fig. 7. Calculations of magnetic field gradient plotted along the *y*-axis showed a very large gradient above the central interface between the two magnets. It is caused by a very significant change of field magnitude along a very short distance of an order of 200–300 μm. Also, large (however, much smaller than above the central interface line) gradients exist on both magnets' edges. In the simulations, we used the same geometry and material parameters of the magnets to match as closely as possible the experimental magnet sizes and their ferromagnetic parameters, such as remanence and coercivity. To maximize influence of the magnetic field, we placed magnets very close to the cells. This was achieved by constructing the slide chamber with a microscope cover glass at the bottom.

The most pronounced changes in macrophage shape and alignment were observed in two characteristic locations, marked as regions #1 and #2 in Fig. 7. The first region is located above the central maximum gradient line between two magnets, and the latter region is located close to the magnet corner, where two magnetic force components perpendicular to each other were identified. Such perpendicular forces were created due to the magnets' edge-introduced gradients. As the reference with no magnetic field present, an area outside the magnets, marked as region #3 in Fig. 7, was selected. The highest concentration of elongated macrophages was observed in the vicinity of the maximum gradient line and also along a diagonal line of the magnets at their corners.

At the interface, the elongated macrophages grouped along the maximum gradient line were aligned perpendicular to the direction to the magnetic gradient-generated force vectors, as shown in region #1 in Figs. 7 and 8. At the same time in region #2 (Figs. 7 and 8), long-range, well-aligned macrophages were observed at the corners along the diagonal lines of both magnets. Macrophages that are close to magnet corners are exposed to two nonuniform magnetic field-generated forces perpendicular to each other.

If an object is placed in a magnetic field of strength H, its magnetic response will lead to magnetization, which for diamagnetic and paramagnetic materials is linearly proportional to H ($M = \chi H$, where χ is magnetic susceptibility). Biological

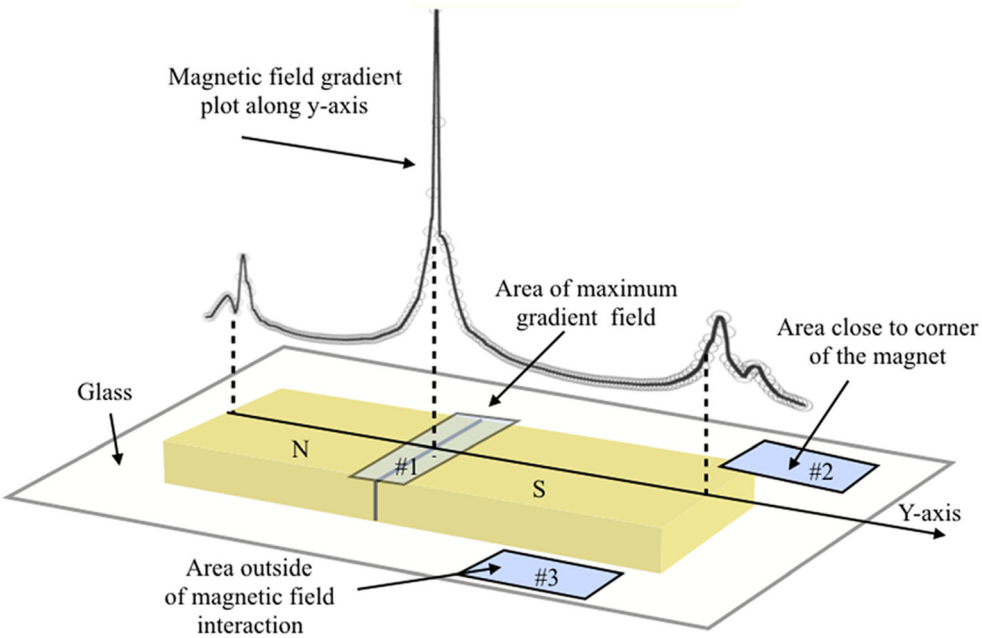

Fig. 7 A sketch describing an experimental configuration of two permanent magnets covered by a very thin glass plate. A sketch describing an experimental configuration of two permanent magnets covered by a very thin glass plate is presented. The magnetic field gradient calculated along the *y*-axis is plotted. Three of the most characteristic areas above the magnets, where highly elongated, elongated/long-range aligned, and magnetic field-unaffected macrophages were observed, are marked as regions #1, #2, and #3, respectively

cells are mostly diamagnetic, usually with a small negative magnetic susceptibility. In a uniform magnetic field, such cells will be repelled, in contrast to the paramagnetic materials, which have a positive magnetic susceptibility and, as a result, they will be attracted to the magnetic field lines. However, in a uniform field, neither diamagnetic nor paramagnetic cells will experience translational force; they will only be disturbing field homogeneity. The translational force (F_{mag}) exists in such a system but only in a nonuniform magnetic field, and it will be moving diamagnetic or paramagnetic cells from a strong to a weak field and in a reverse direction, respectively. If cells are placed in a buffer medium, which can be either dia- or paramagnetic, the response of cells to the magnetic field gradient will depend on the difference between cell and medium susceptibilities [43, 44] and it can be expressed as:

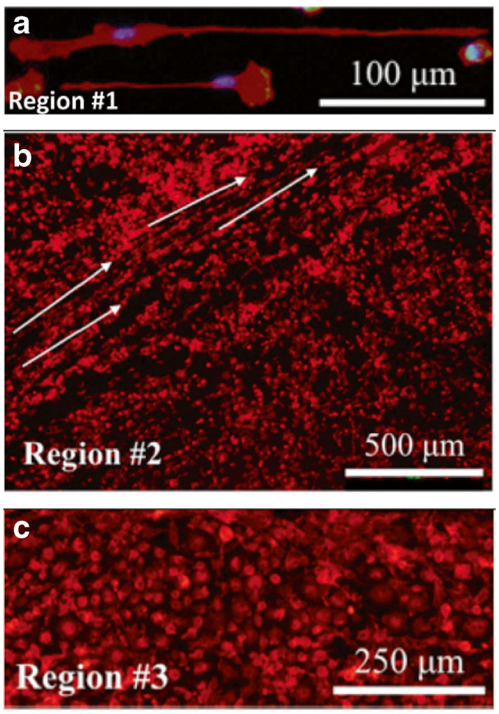

Fig. 8 Characteristic regions where macrophages were investigated. Region #1 (**a**) refers to the interface where the maximum of the gradient was created, region #2 (**b**) marks an area close to the magnet corners along the diagonal line of the whole structure, and region #3 (**c**) marks an area outside the magnetic field interaction

$$\overrightarrow{F_{\mathrm{mag}}} = \frac{\Delta\chi V}{\mu_0}\left(\vec{B}\cdot\nabla\vec{B}\right), \tag{1}$$

where B is the magnetic induction, ∇ is the nabla operator, V is the volume of the cell, μ_0 is the permeability of the free space, and $\Delta\chi = \chi_c - \chi_M$ is the magnetic susceptibility difference between the cell and surrounding buffer medium. As can be seen from this equation, the magnetic force is dependent on the product of the magnetic induction B (in T units) with the magnetic field gradient (in T/m). Since it is directly proportional to the product of the two, it is often referred to as the "force product," and it is given in T^2/m units. The close-to-interface gradient magnitude is in our case 10^4 T/m, which is smaller than gradients achieved for periodically patterned structures [45–47]. In general, as it is sketched in Fig. 9a, b, on the cells in a buffer media layer besides magnetic force (F_{mag}) a buoyancy force (F_b) also acts, which can be expressed [48] as

$$\overrightarrow{F_b} = V\Delta\rho\vec{g}, \tag{2}$$

where g is the gravitational acceleration in z-direction and ρ is the difference between the volumetric densities of the cell

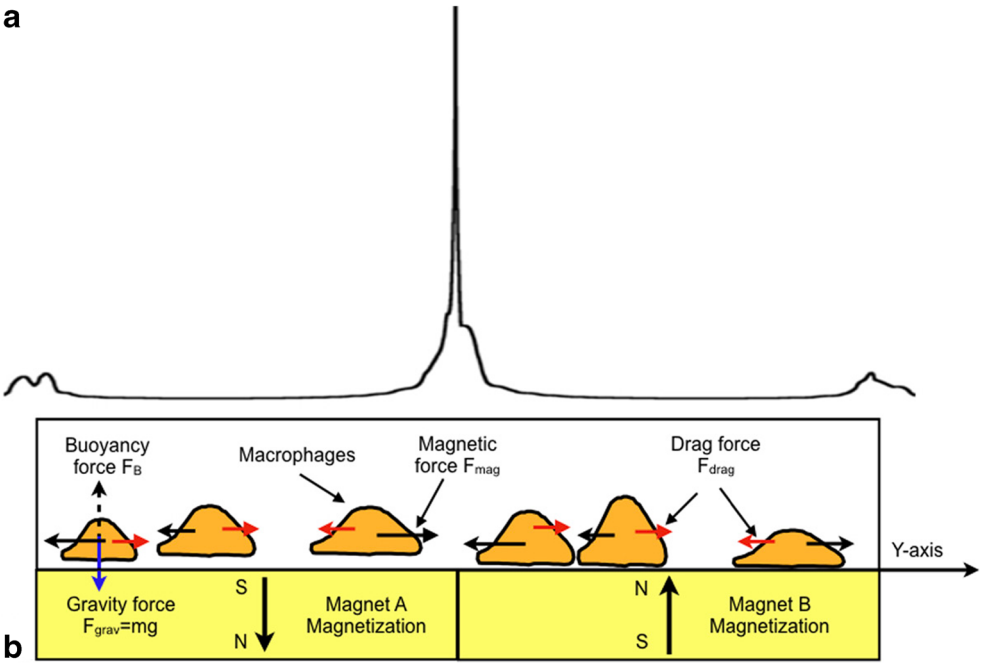

Fig. 9 Forces acting on macrophages placed in magnetic field. Magnetic (F_{mag}, black arrow), gravity (F_{grav}, blue arrow), buoyancy (F_B, dashed arrow), and drag (F_{drag}, red arrow) forces exerted to cells due to the presence of the magnetic field gradient, gravity, and surrounding cell media. N-S anti-parallel arrangement of two magnets is shown, and magnetic force F_{mag} along the y-axis is plotted to show where the strongest force above the two magnets exists

and the buffer medium. Also during the cell movement, it will gain a velocity v and drag force F_d will be exerted on the cell. Such force for a spherical object be calculated [49, 50] from the following equation:

$$\overrightarrow{F_d} = 6\pi f_D R\eta \overrightarrow{v}, \quad (3)$$

where R is the radius of the cell, η is the dynamic viscosity of the buffer medium, and f_D is the drag coefficient, which is equal to 1 when the cell is distant from the container boundary.

Equation 1 shows that for positive $\Delta\chi$, the cells will be drawn to the lines of the highest gradient, whereas for the negative sign, the cells will be repulsed. Our experiments showed that, indeed, cells are attracted to the highest gradient (Fig. 7), where the strongest gradient area (region #1) coincides with the area where higher density and elongated macrophages were observed.

We have simulated the movement of the cells for two directions of the F_{mag} (Eq. 1) force determined by either positive or negative signs of $\Delta\chi$ susceptibility difference. Macrophages were represented by spherical particles. Mass of each particle was selected to match the mass of a macrophage and was in the order of 70–80 × 10^{-12} g [51]. We have found that the calculated pattern of magnetic field-induced force vectors induced by magnets explain very well the observed alignment and distribution of elongated macrophages. In the simulation, we used ANSYS (Maxwell) [42] and visual molecular dynamics (VMD) [52] software packages. Maxwell allowed us to calculate the magnetic field generated by the two magnets and the corresponding vector field distribution of the magnetic force. We limited movement freedom of spherical particles to a 2D case, and, in addition, to simplify the calculation problem, both viscosity and gravity effects were ignored. In our molecular dynamic simulation initially at $t = 0$ (Figs. 10a and 11a), we considered 100 equally spaced, thus covering uniformly the whole magnets' area particles and no magnetic field present. When there is no magnetic field-generated force, the particles are not subjected to any force. We have neglected Brownian force for this case because it is much smaller than magnetic field-related force. However, when a nonuniform magnetic field generated by underlying magnets was applied, the particles were moved on trajectories that follow the lines of the magnetic force vectors. Figures 10 and 11b–d show the particles' distribution at three time points. We carried out a simulation for 20 × 10^6 steps, where each step was set as 0.005 s, and the initial velocity (at $t = 0$) was set to zero.

The final trajectories of particles under applied magnetic field forces can be visualized from Figs. 10 and 11, where the cases of repelling from and attracting to the highest gradient lines are presented, respectively. The highest density of elongated macrophages above the magnets' interface line observed in our experiments indicates that the $\Delta\chi$ is positive because of higher susceptibility of macrophages than the medium.

Also, observed attraction of macrophages to the highest gradient areas allows the conclusion to be drawn that in our experiments, the cells are less diamagnetic than the medium.

In Fig. 10, where the case of $\Delta\chi < 0$ is depicted, the cells are repelled from the area of the highest gradient, which should result in no cells above the interface area because they will be pushed to the lowest or no-gradient areas. When $\Delta\chi >$ 0, the cells will be aligned along the lines of the high gradient.

Comparison of macrophage morphology showed that control macrophages grown without the magnet were uniformly distributed and only slightly elongated (average length around 50 μm;

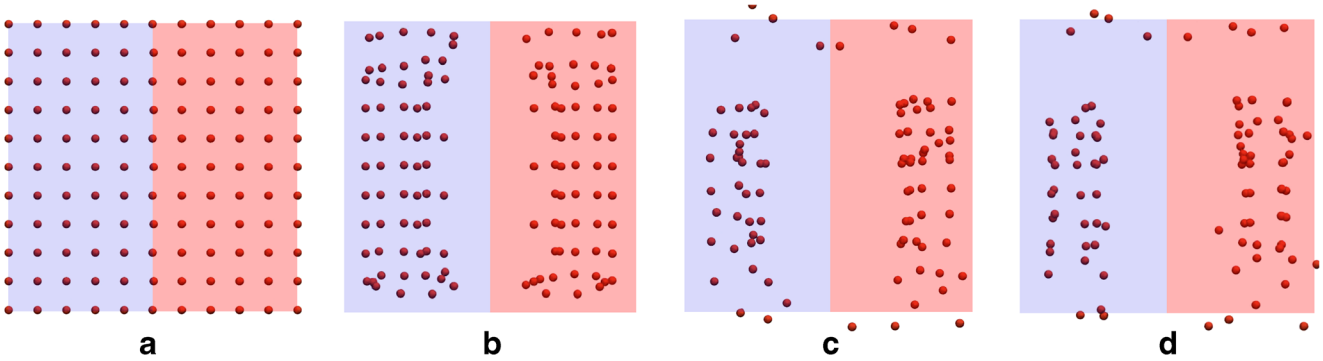

Fig. 10 For $\Delta\chi$, negative macrophages are repelled from the highest gradient areas. Simulated distribution of the cells located above two magnets and exposed to nonuniform magnetic field as a function of time. Negative sign of $\Delta\chi$ was assumed. It describes the following cases: **a** no magnetic field applied and uniform initial distribution assumed, **b** magnetic field applied and the cells are repelled from the highest gradient lines located above the interface between the magnets and above magnet edges, **c** magnetic field applied for longer than in **b** case time, and **d** magnetic field is still applied and quasi equilibrium is achieved

Fig. 8c). In contrast, macrophages grown in the presence of magnets aggregated along the interface between two magnets, and they were extremely elongated (average length exceeding 150 μm; Fig. 8a). The shape and elongation of these macrophages were very similar to the RhoA-deleted or RhoA/ROCK-inhibited hummingbird phenotype macrophages.

In addition, we observed that macrophages grown on magnets were distributed in distinct columns/rows (Fig. 8b). Similar columns of cells were observed in the wound-healing studies, where the fibroblasts were elongated and arranged in columns consisting of leader cells and following cells [53, 54]. These studies showed that, within each column, the first cell that had re-arranged its actin cytoskeleton and elongated was the leader cell. Subsequently, the changes in the actin cytoskeleton of the leader cell provoked the changes in the following cells and caused a directional movement of all cells within the column. By analogy, it is possible that a similar principle directs formation of the columns/rows of macrophages in response to the magnetic field. We also observed that the elongated macrophages were aligned according to the magnetic forces' pattern (Fig.8a). We believe that this occurred because the elongated macrophages have high diamagnetic anisotropy and, thus, are susceptible to the rotational magnetic field-driven forces.

The observation that the magnetic field exposure changes the shape of macrophages agrees with published observations that the mechanical stress applied externally on the cell modifies visco-elastic properties of the cell cytoskeleton [49, 50, 55]. The question arises how the externally applied magnetic field can change the organization of the intracellular cytoskeleton. The results of our study indicate that this happens through changes in the ionic current and distortion of the cell membrane. The influence of static magnetic fields on cell morphology, cell membrane, and level of intracellular Ca^{2+} has been observed previously in lymphocytes and human lung (lymphoblast) U937 cells [56].

We showed that the macrophages exposed to the magnetic field clustered the cation channel receptors TRPM2, which are responsible for Ca^{+2} homeostasis, and probably made them nonfunctional. Because actin polymerization is ion current- and Ca^{+2}-dependent, this affected actin polymerization and resulted in macrophage elongation. We observed also that RhoA-deleted macrophages had similar clustering of the receptors; in this case, these were the CX3CR1 receptors, which are responsible for the macrophage movement to the source of the inflammation/transplanted organ [35]. We showed previously that, when the naïve M0 macrophage polarizes into M2

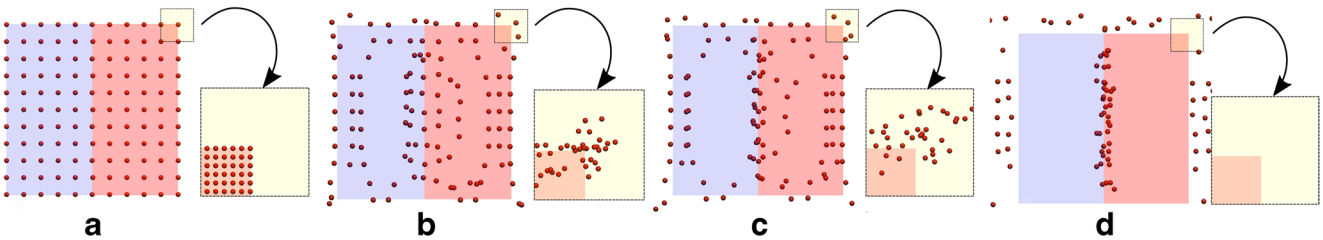

Fig. 11 For $\Delta\chi$, positive macrophages are attracted to the highest gradient areas. Simulated distribution of cells placed above the magnets as a function of time for positive sign of $\Delta\chi$. In contrary to the case shown in Fig. 10, the cells' movement demonstrates that they are attracted to the highest gradient lines (interface between and edges of the two magnets). The following cases were considered: **a** no magnetic field applied with initial uniform density of the cells, **b** magnetic field applied and the cells are attracted to the highest gradient areas, **c** magnetic field is applied longer than in case **b**, and **d** magnetic field applied and equilibrium is reached. Macrophages in the magnet corner areas are subjected to two magnetic field-generated forces perpendicular to each other. This results in "leaking" of the cells outside the magnets' area along a diagonal direction, as shown in insets. One of the magnet corners is marked with a square, and insets depict "leaking" of the cells' dynamic

phenotype, they elongate and start expression of the M2-specific genes [10–12, 35]. This suggests that the magnetic field-enforced elongation may also turn on the expression of M2-specific genes in the macrophages.

This magnetically induced, elongated M2-like phenotype of macrophages is very similar to the phenotype achieved by pharmacological (Y27632 inhibitor) or genetic (macrophage-specific deletion of RhoA) manipulation of the RhoA pathway [10–12, 35]. This suggests that, after further in vitro and in vivo studies, the magnetic field-gradient methodology may be a novel approach to influence macrophage phenotype and functions.

Although the RhoA-deleted and magnet-grown macrophages have a very similar elongated, hummingbird phenotype, there are also important differences, indicating a difference in the mechanism(s) underlying the elongation phenomenon. In the RhoA-deleted or RhoA-inhibitor-treated macrophages, the focal adhesions accumulated in the macrophage tail. This prevented detachment of the macrophage tail from the substrate, while the front of the macrophage moved forward [35]. In contrast, in the macrophages exposed to the magnetic field, the focal adhesions did not accumulate in the tail [41]. Also, the effects of RhoA deletion and magnetic interference on the macrophage Golgi complex were different. While RhoA deletion caused reduction in the number and size of Golgi cisternae, the magnetic interference caused dispersion of the Golgi [35, 41]. These differences indicate that the mechanism(s) underlying the changes in the actin cytoskeleton induced by RhoA-deletion and magnetic interference must be profoundly different. Further studies are needed to shed more light on the effect of the magnetic field on the macrophage actin cytoskeleton.

In summary, we showed that the magnetic field disrupted the actin filament cytoskeleton in the macrophages, which in turn caused macrophage elongation and interfered with the organization of the Golgi complex and receptors. All these changes imitated the effect of the deletion of RhoA in the macrophages.

Conclusions

The data presented above indicate that bioengineering of the shape of immune cells such as macrophages using genetic, pharmacologic, or mechanical/magnetic interference with cellular cytoskeleton profoundly affects macrophage functions and prevents them from mounting an immune response. Because genetic interference cannot be applied to humans and drug/inhibitors are very often toxic and not approved for clinical use, magnetic bioengineering has the potential to be used in development of novel anti-rejection therapies in clinical organ transplantation. In addition, because cancer cell motility and divisions also depend on the cellular cytoskeleton, this novel methodology has the potential to be used in designing anti-cancer and anti-metastatic therapies.

Recent in vitro studies showed that there is very clear interaction between cells and the magnetic field [44, 45, 57], and that the uniform and nonuniform field forces affect all aspects of cell structure, differentiation, and behavior [57, 58]. In addition, it has been shown that the magnetic field gradients and microgravity effects are very similar [59–61]. One of the ways to increase the effect of magnetic force on cells is to make the environment more paramagnetic. The example is the use of contrasting agents such as gadolinium in the magnetic resonance imaging, which, because of its paramagnetic properties, increases the magnetic force effect on cells [57]. It is known that the rearrangements of cellular cytoskeleton, which occur in cancer cells, result in increased cell migration and cancer metastasis. Thus, similar to the macrophages, the magnetic field interference may potentially be adapted to change the cytoskeleton and behavior of cancer cells.

Acknowledgments The authors gratefully acknowledge the support from the William and Ella Owens Medical Research Foundation, the William Stamps Farish Fund, and the State of Texas through the Texas Center for Superconductivity at the University of Houston.

Compliance with ethical standards

Conflict of interest The authors declare that they have no conflict of interest.

References

1. Lee M, Vasioukhin V. Cell polarity and cancer—cell and tissue polarity as a non-canonical tumor suppressor. J Cell Sci. 2008;121(Pt 8):1141–50. https://doi.org/10.1242/jcs.016634.
2. Geissmann F, Manz MG, Jung S, Sieweke MH, Merad M, Ley K. Development of monocytes, macrophages, and dendritic cells. Science. 2010;327(5966):656–61. https://doi.org/10.1126/science.1178331.
3. Kloc M, Li X, Ghobrial R. Are macrophages responsible for cancer metastasis? J Immuno Biol. 2016;1:103. https://doi.org/10.4172/jib.1000103.
4. Murray PJ, Wynn TA. Protective and pathogenic functions of macrophage subsets. Nat Rev Immunol. 2011;11(11):723–37. https://doi.org/10.1038/nri3073.
5. Kloc M, Ghobrial RM. Chronic allograft rejection: a significant hurdle to transplant success. Burns Trauma. 2014;2(1):3–10. https://doi.org/10.4103/2321-3868.121646.
6. Kloc M, Li X, Ghobrial RM. RhoA cytoskeletal pathway to transplantation. J Immun Clincal Res. 2014;2:1012–6.
7. Liu Y, Kloc M, Li XC. Macrophages as effectors of acute and chronic allograft injury. Curr Transplant Rep. 2016;3(4):303–12. https://doi.org/10.1007/s40472-016-0130-9.
8. Kaul AM, Goparaju S, Dvorina N, Iida S, Keslar KS, de la Motte CA, et al. Acute and chronic rejection: compartmentalization and kinetics of counterbalancing signals in cardiac transplants. Am J Transplant. 2015;15(2):333–45. https://doi.org/10.1111/ajt.13014.

9. Hettinger J, Richards DM, Hansson J, Barra MM, Joschko AC, Krijgsveld J, et al. Origin of monocytes and macrophages in a committed progenitor. Nat Immunol. 2013;14(8):821–30. https://doi.org/10.1038/ni.2638.
10. Liu Y, Minze LJ, Mumma L, Li XC, Ghobrial RM, Kloc M. Mouse macrophage polarity and ROCK1 activity depend on RhoA and non-apoptotic caspase 3. Exp Cell Res. 2016;341(2):225–36. https://doi.org/10.1016/j.yexcr.2016.02.004.
11. Liu Y, Tejpal N, You J, Li XC, Ghobrial RM, Kloc M. ROCK inhibition impedes macrophage polarity and functions. Cell Immunol. 2016;300:54–62. https://doi.org/10.1016/j.cellimm.2015.12.005.
12. Liu Y, Chen W, Minze LJ, Kubiak JZ, Li XC, Ghobrial RM, et al. Dissonant response of M0/M2 and M1 bone-marrow-derived macrophages to RhoA pathway interference. Cell Tissue Res. 2016;366:707–20. https://doi.org/10.1007/s00441-016-2491-x.
13. Liu Y, Kubiak JZ, Li XC, Ghobrial RM, Kloc M. Macrophages and RhoA pathway in transplanted organs. Results Probl Cell Differ. 2017;62:365–76. https://doi.org/10.1007/978-3-319-54090-0_15.
14. McWhorter FY, Wang T, Nguyen P, Chung T, Liu WF. Modulation of macrophage phenotype by cell shape. Proc Natl Acad Sci U S A. 2013;110(43):17253–8. https://doi.org/10.1073/pnas.1308887110.
15. Artemenko Y, Axiotakis L Jr, Borleis J, Iglesias PA, Devreotes PN. Chemical and mechanical stimuli act on common signal transduction and cytoskeletal networks. Proc Natl Acad Sci U S A. 2016;113(47):E7500–E9. https://doi.org/10.1073/pnas.1608767113.
16. Lin BH, Tsai MH, Lii CK, Wang TS. IP3 and calcium signaling involved in the reorganization of the actin cytoskeleton and cell rounding induced by cigarette smoke extract in human endothelial cells. Environ Toxicol. 2016;31(11):1293–306. https://doi.org/10.1002/tox.22133.
17. Cunniff B, McKenzie AJ, Heintz NH, Howe AK. AMPK activity regulates trafficking of mitochondria to the leading edge during cell migration and matrix invasion. Mol Biol Cell. 2016;27(17):2662–74. https://doi.org/10.1091/mbc.E16-05-0286.
18. Mehta MM, Weinberg SE, Chandel NS. Mitochondrial control of immunity: beyond ATP. Nat Rev Immunol. 2017;17(10):608–20. https://doi.org/10.1038/nri.2017.66.
19. Schuler MH, Lewandowska A, Caprio GD, Skillern W, Upadhyayula S, Kirchhausen T, et al. Miro1-mediated mitochondrial positioning shapes intracellular energy gradients required for cell migration. Mol Biol Cell. 2017;28(16):2159–69. https://doi.org/10.1091/mbc.E16-10-0741.
20. Wheeler AP, Ridley AJ. Why three Rho proteins? RhoA, RhoB, RhoC, and cell motility. Exp Cell Res. 2004;301(1):43–9. https://doi.org/10.1016/j.yexcr.2004.08.012.
21. Bos N, Zimmerman A, Olson J, Yew J, Yerkie J, Dahl E, et al. From shared databases to communities of practice: a taxonomy of collaboratories. J Computer-Mediated Comm. 2007;12(2):652–72. https://doi.org/10.1111/j.1083-6101.2007.00343.x.
22. Cherfils J, Zeghouf M. Regulation of small GTPases by GEFs, GAPs, and GDIs. Physiol Rev. 2013;93(1):269–309. https://doi.org/10.1152/physrev.00003.2012.
23. Dubash AD, Wennerberg K, Garcia-Mata R, Menold MM, Arthur WT, Burridge K. A novel role for Lsc/p115 RhoGEF and LARG in regulating RhoA activity downstream of adhesion to fibronectin. J Cell Sci. 2007;120(Pt 22):3989–98. https://doi.org/10.1242/jcs.003806.
24. Shang X, Marchioni F, Sipes N, Evelyn CR, Jerabek-Willemsen M, Duhr S, et al. Rational design of small molecule inhibitors targeting RhoA subfamily Rho GTPases. Chem Biol. 2012;19(6):699–710. https://doi.org/10.1016/j.chembiol.2012.05.009.
25. Shang X, Marchioni F, Evelyn CR, Sipes N, Zhou X, Seibel W, et al. Small-molecule inhibitors targeting G-protein-coupled Rho guanine nucleotide exchange factors. Proc Natl Acad Sci U S A. 2013;110(8):3155–60. https://doi.org/10.1073/pnas.1212324110.
26. Goode BL, Eskin JA, Wendland B. Actin and endocytosis in budding yeast. Genetics. 2015;199(2):315–58. https://doi.org/10.1534/genetics.112.145540.
27. Egea G, Serra-Peinado C, Gavilan MP, Rios RM. Cytoskeleton and Golgi-apparatus interactions: a two-way road of function and structure. Cell Health Cytosk. 2015:37. https://doi.org/10.2147/chc.s57108.
28. Marra P, Salvatore L, Mironov A Jr, Di Campli A, Di Tullio G, Trucco A, et al. The biogenesis of the Golgi ribbon: the roles of membrane input from the ER and of GM130. Mol Biol Cell. 2007;18(5):1595–608. https://doi.org/10.1091/mbc.E06-10-0886.
29. Maxfield FR, McGraw TE. Endocytic recycling. Nat Rev Mol Cell Biol. 2004;5(2):121–32. https://doi.org/10.1038/nrm1315.
30. Prosser DC, Wendland B. Conserved roles for yeast Rho1 and mammalian RhoA GTPases in clathrin-independent endocytosis. Small GTPases. 2012;3(4):229–35. https://doi.org/10.4161/sgtp.21631.
31. Rossanese O, Reinke C, Bevis B, Hammond A, Sears I, O'Connor J, et al. A role for actin, Cdc1p, and Myo2p in the inheritance of late Golgi elements in Saccharomyces cerevisiae. J Cell Biol. 2001;153(1):47–62.
32. Zilberman Y, Alieva NO, Miserey-Lenkei S, Lichtenstein A, Kam Z, Sabanay H, et al. Involvement of the Rho-mDia1 pathway in the regulation of Golgi complex architecture and dynamics. Mol Biol Cell. 2011;22(16):2900–11. https://doi.org/10.1091/mbc.E11-01-0007.
33. Meunier FA, Gutierrez LM. Captivating new roles of F-actin cortex in exocytosis and bulk endocytosis in neurosecretory cells. Trends Neurosci. 2016;39(9):605–13. https://doi.org/10.1016/j.tins.2016.07.003.
34. Mori TTK, Naito M, Kodama T, Hakamata H, Sakai M, Miyazaki A, et al. Endocytic pathway of scavenger receptors via trans-Golgi system in bovine alveolar macrophages. Lab Investig. 1994;71(3):409–16.
35. Liu Y, Chen W, Wu C, Minze LJ, Kubiak JZ, Li XC et al. Macrophage/monocyte-specific deletion of Ras homolog gene family member A (RhoA) downregulates fractalkine receptor and inhibits chronic rejection of mouse cardiac allografts. J Heart Lung Transpl. 2016:30292–3. https://doi.org/10.1016/j.healun.2016.08.011.
36. Chen W, Zhao Y, Li XC, Kubiak JZ, Ghobrial RM, Kloc M. Rho-specific guanine nucleotide exchange factors (Rho-GEFs) inhibition affects macrophage phenotype and disrupts Golgi complex. Int J Biochem Cell Biol. 2017;93:12–24. https://doi.org/10.1016/j.biocel.2017.10.009.
37. Porat-Shliom N, Weigert R, Donaldson JG. Endosomes derived from clathrin-independent endocytosis serve as precursors for endothelial lumen formation. PLoS One. 2013;8(11):e81987. https://doi.org/10.1371/journal.pone.0081987.
38. Lee K, Kim EH, Oh N, Tuan NA, Bae NH, Lee SJ, et al. Contribution of actin filaments and microtubules to cell elongation and alignment depends on the grating depth of microgratings. J Nanobiotechnology. 2016;14(1):35. https://doi.org/10.1186/s12951-016-0187-8.
39. Lee CH, Kim YJ, Jang JH, Park JW. Modulating macrophage polarization with divalent cations in nanostructured titanium implant surfaces. Nanotechnology. 2016;27(8):085101. https://doi.org/10.1088/0957-4484/27/8/085101.
40. Wang T, Luu TU, Chen A, Khine M, Liu WF. Topographical modulation of macrophage phenotype by shrink-film multi-scale wrinkles. Biomater Sci. 2016;4(6):948–52. https://doi.org/10.1039/c6bm00224b.
41. Wosik J, Chen W, Qin K, Ghobrial RM, Kubiak JZ, Kloc M. Magnetic field changes macrophage phenotype. Biophys J. 2018;114(8):2001–13. https://doi.org/10.1016/j.bpj.2018.03.002.
42. ANSYS, Maxwell. http://ansoft-maxwell.narod.ru/en/Maxwell_v16_L01_Introduction.pdf. Accessed 21 May 2013.
43. Eguchi Y, Ueno S, Kaito C, Sekimizu K, Shiokawa K. Cleavage and survival of Xenopus embryos exposed to 8 T static magnetic fields in a rotating clinostat. Bioelectromagnetics. 2006;27(4):307–13. https://doi.org/10.1002/bem.20215.

44. Denegre JM, Valles JM Jr, Lin K, Jordan WB, Mowry KL. Cleavage planes in frog eggs are altered by strong magnetic fields. Proc Natl Acad Sci U S A. 1998;95(25):14729–32.
45. Kauffmann P, Ith A, O'Brien D, Gaude V, Boue F, Combe S, et al. Diamagnetically trapped arrays of living cells above micromagnets. Lab Chip. 2011;11(18):3153–61. https://doi.org/10.1039/c1lc20232d.
46. Gassner AL, Abonnenc M, Chen HX, Morandini J, Josserand J, Rossier JS, et al. Magnetic forces produced by rectangular permanent magnets in static microsystems. Lab Chip. 2009;9(16):2356–63. https://doi.org/10.1039/b901865d.
47. Zablotskii V, Pastor JMn, Larumbe S, Pérez-Landazábal JI, Recarte V, Gómez-Polo C et al. High-field gradient permanent micromagnets for targeted drug delivery with magnetic nanoparticles. 2010:152–157. doi:https://doi.org/10.1063/1.3530005.
48. Gijs MA, Lacharme F, Lehmann U. Microfluidic applications of magnetic particles for biological analysis and catalysis. Chem Rev. 2010;110(3):1518–63. https://doi.org/10.1021/cr9001929.
49. Ghibaudo M, Trichet L, Le Digabel J, Richert A, Hersen P, Ladoux B. Substrate topography induces a crossover from 2D to 3D behavior in fibroblast migration. Biophys J. 2009;97(1):357–68. https://doi.org/10.1016/j.bpj.2009.04.024.
50. Ladoux B, Nicolas A. Physically based principles of cell adhesion mechanosensitivity in tissues. Rep Prog Phys. 2012;75(11):116601. https://doi.org/10.1088/0034-4885/75/11/116601.
51. Bryan AK, Hecht VC, Shen W, Payer K, Grover WH, Manalis SR. Measuring single cell mass, volume, and density with dual suspended microchannel resonators. Lab Chip. 2014;14(3):569–76. https://doi.org/10.1039/c3lc51022k.
52. Humphrey W, Dalke A, Schulten K. VMD: visual molecular dynamics. J Mol Graph. 1996;14(1):33–8. https://doi.org/10.1016/0263-7855(96)00018-5.
53. Omelchenko T, Vasiliev JM, Gelfand IM, Feder HH, Bonder EM. Rho-dependent formation of epithelial "leader" cells during wound healing. Proc Natl Acad Sci U S A. 2003;100(19):10788–93. https://doi.org/10.1073/pnas.1834401100.
54. Gov NS. Collective cell migration patterns: follow the leader. Proc Natl Acad Sci U S A. 2007;104(41):15970–1. https://doi.org/10.1073/pnas.0708037104.
55. Qian A-R, Gao X, Zhang W, Li J-B, Wang Y, Di S-M, et al. Large gradient high magnetic fields affect osteoblast ultrastructure and function by disrupting collagen I or fibronectin/αβ1 integrin. PLoS One. 2013;8(1):e51036.
56. Chionna A, Dwikat M, Panzarini E, Tenuzzo B, Carla EC, Verri T, et al. Cell shape and plasma membrane alterations after static magnetic fields exposure. Eur J Histochem. 2003;47(4):299–308.
57. Winkleman A, Gudiksen KL, Ryan D, Whitesides GM, Greenfield D, Prentiss M. A magnetic trap for living cells suspended in a paramagnetic buffer. Appl Phys Lett. 2004;85(12):2411–3. https://doi.org/10.1063/1.1794372.
58. Shi D, Meng R, Deng W, Ding W, Zheng Q, Yuan W, et al. Effects of microgravity modeled by large gradient high magnetic field on the osteogenic initiation of human mesenchymal stem cells. Stem Cell Rev Rep. 2010;6(4):567–78.
59. Beaugnon E, Tournier R. Levitation of organic materials. Nature. 1991;349(6309):470.
60. Kuznetsov OA, Hasenstein KH. Intracellular magnetophoresis of amyloplasts and induction of root curvature. Planta. 1996;198(1):87–94.
61. Yamaguchi M, Tanimoto Y. Magneto-science: magnetic field effects on materials: fundamentals and applications, Springer Series in Materials Science, Volume 89 ISBN 978-3-540-37061-1 Kodansha Ltd and Springer-Verlag Berlin Heidelberg, 2006. 2006;1.